THE NATURE OF THE $X(2175)$*

S. Coito, G. Rupp

Centro de Física das Interacções Fundamentais, Instituto Superior Técnico
Technical University of Lisbon, 1049-001 Lisboa, Portugal

E. van Beveren

Centro de Física Computacional, Departamento de Física
Universidade de Coimbra, 3004-516 Coimbra, Portugal

(Received October 2, 2009)

We study the puzzling vector meson $X(2175)$ in a multichannel generalisation of the Resonance Spectrum Expansion model. Besides the usual P-wave pseudoscalar–pseudoscalar, pseudoscalar–vector, and vector–vector channels that couple to mesons with vector quantum numbers, we also include the important S-wave vector–scalar, pseudoscalar–axial-vector and vector–axial-vector channels, including the observed $\phi(1020)\,f_0(980)$ decay mode. The strong coupling to nearby S-wave channels originate dynamically generated poles, two of which come out close to the energy region of the $X(2175)$, *viz.* at $(2.037-i0.170)$ GeV and $(2.382-i0.20)$ GeV. Further improvements are proposed.

PACS numbers: 14.40.Cs, 11.80.Gw, 11.55.Ds, 13.75.Lb

1. Introduction

The $X(2175)$ was first observed by BABAR [1] in the process $e^+e^- \to \phi(1020)f_0(980)$, and identified as a 1^{--} resonance, with $M = (2.175\pm0.010\pm 0.015)\,\mathrm{GeV}$ and $\Gamma = (58 \pm 16 \pm 20)$ MeV. This state was then confirmed by BES and denoted $Y(2175)$ [2], from the decay $J/\Psi \to \eta\phi f_0(980)$, with $M = (2.186 \pm 0.010 \pm 0.006)\,\mathrm{GeV}$ and $\Gamma = (65 \pm 25 \pm 17)\,\mathrm{MeV}$. It is now included in the PDG Particle Listings [3] as the $\phi(2170)$.

On the theoretical side, the $X(2175)$ has been described as a three-meson resonance in a Faddeev calculation for the $\phi K\bar{K}$ system [4], obtaining a narrow peak around 2150 MeV, about 27 MeV wide. Earlier, a conventional Resonance Chiral Perturbation Theory calculation [5] failed to produce such

* Presented at the International Meeting "Excited QCD", Zakopane, Poland, February 8–14, 2009.

a peak, which led to the former 3-body model. Other approaches include QCD-sum rule calculations for a tetra quark state [6], and a perturbative multichannel analysis to distinguish between a strangeonium hybrid and a normal $2\,^3D_1$ $s\bar{s}$ state [7].

2. Resonance spectrum expansion and the $X(2175)$

In the present study of the $X(2175)$, we use the Resonance Spectrum Expansion (RSE) model [8] to unitarise a normal $s\bar{s}$ spectrum. In the RSE approach, non-exotic mesons are described as regular quark–antiquark states, but non-perturbatively dressed with meson–meson components. An important feature is the inclusion of a complete $q\bar{q}$ confinement spectrum in the intermediate state [8, 9], resulting for the multichannel case in an effective meson–meson potential

$$V_{ij}^{(L_i,L_j)}(p_i,p'_j;E) = \lambda^2\, j^i_{L_i}(p_i a)\, j^j_{L_j}(p'_j a) \sum_{n=0}^{\infty} \frac{g_i(n) g_j(n)}{E - E_n}\ , \tag{1}$$

where λ is an overall coupling constant, a a parameter mimicking the average string-breaking distance, $j^i_{L_i}$ a spherical Bessel function, p_i and p'_j the relativistically defined relative momenta of initial channel i and final channel j, respectively, $g_i(n)$ the coupling of channel i to the n-th $q\bar{q}$ recurrence, and E_n the discrete energy of the latter confinement state. Note that the couplings $g_i(n)$, evaluated on a harmonic oscillator (HO) basis for the $^3P_0$ model [10], decrease very rapidly for increasing n, so that practical convergence is achieved with the first 20 terms in the infinite sum. Moreover, the separable form of the effective potential (1) allows the solution of the (relativistic) Lippmann–Schwinger equation in closed form.

In the present first study, we restrict ourselves to the $^3S_1$ channel for the $q\bar{q}$ system. Moreover, we assume ideal mixing, so that only $s\bar{s}$ states are considered. For the confinement mechanism, we take an HO potential. This choice is not strictly necessary, as Eq. (1) allows for any confinement spectrum, but the HO has shown to work fine in practically all phenomenological applications. The flavour-dependent HO spectrum reads

$$E_n = m_q + m_{\bar{q}} + \omega(2n + \tfrac{3}{2} + \ell)\ . \tag{2}$$

The parameter values $\omega = 190$ MeV and $m_s = 508$ MeV are kept unchanged with respect to all previous work (see *e.g.* Ref. [11]). In Table I, we list some of the eigenvalues given by Eq. (2). As for the decay sector that couples to $J^{\rm PC}=1^{--}$ ϕ states, we take all pseudoscalar–pseudoscalar (PP), pseudoscalar–vector (PV), and vector–vector (VV) channels, which are in P-waves, as well as all vector–scalar (VS), pseudoscalar–axial-vector (PA),

TABLE I

HO eigenvalues (2) in GeV, for $\omega = 190$ MeV, $m_s = 508$ MeV, $\ell = 0$.

n	$s\bar{s}$
0	1.301
1	1.681
2	2.061
3	2.441
4	2.821

and vector–axial-vector (VA) channels, being in S-waves. These 15 channels are listed in Table II, including the observed [1, 2] $\phi f_0(980)$ mode, with the respective orbital angular momenta, spins, and thresholds.

TABLE II

Thresholds in GeV of included meson–meson channels (see Ref. [3]).

Channel	Relative L, total S	Threshold
KK	$1, 0$	0.987
KK^*	$1, 1$	1.388
$\eta\phi$	$1, 1$	1.567
$\eta'\phi$	$1, 1$	1.977
K^*K^*	$1, 0$	1.788
K^*K^*	$1, 2$	1.788
$\phi f_0(980)$	$0, 1$	1.999
$K^*K_0^*(800)$	$0, 1$	1.639
$\eta h_1(1380)$	$0, 1$	1.928
$\eta' h_1(1380)$	$0, 1$	2.338
$KK_1(1270)$	$0, 1$	1.764
$KK_1(1400)$	$0, 1$	1.894
$K^*K_1(1270)$	$0, 1$	2.164
$K^*K_1(1400)$	$0, 1$	2.294
$\phi f_1(1420)$	$0, 1$	2.439

3. Results

As emphasised above, the T-matrix for the effective potential (1) can be solved in closed form. Bound states and resonances correspond to poles of T on the appropriate sheet of the many-sheeted Riemann surface. For the 15 channels considered, there are $2^{15} = 32\,768$ such sheets. However, the relevant poles are in principle those that correspond to relative momenta with negative imaginary parts with respect to open channels, and positive imaginary parts for closed channels. The simplest example of a latter-type pole is a bound state, for which the real part of the momentum is zero.

The only two free parameters of the model, *viz.* λ and a, we fix by demanding that the mass and width of the $\phi(1020)$ be reasonably reproduced. For $\boldsymbol{a = 5.0}\,\text{GeV}^{-1}$ and $\boldsymbol{\lambda = 3.75}\,\text{GeV}^{-3/2}$ we get a theoretical pole position of $\boldsymbol{E_{theor} = (1.0145 - i0.0034)}\,\text{GeV}$, to be compared with the PDG [3] value $\boldsymbol{E_{exp} = (1.0195 - i0.0021)}\,\text{GeV}$, which is more than good enough for the present simplified investigation. Of course, besides the $\phi(1020)$, there are several other resonance poles, which are given in Table III, for energies up to about 2.5 GeV[1]. Confinement poles are those that end up at the energies of the confinement spectrum in the limit $\lambda \to 0$. These usually have small to moderate imaginary parts. On the other hand, the continuum poles, which are dynamically generated, disappear in the complex energy plane for $\lambda \to 0$, with $\Im\text{m}E \to -\infty$. The latter poles mostly have large imaginary parts, for physical values of λ, but there are exceptions, like the fifth pole in Table III.

TABLE III

Pole positions, in GeV.

Re	Im	Type of pole
1.0145	−0.0034	confinement, $n = 0$
1.457	−0.011	confinement, $n = 1$
1.980	−0.010	confinement, $n = 2$
2.037	−0.170	continuum
2.382	−0.020	continuum
2.580	−0.123	continuum

Typical cases of pole trajectories are shown in Fig. 1, with the $n=2$ confinement pole in the left-hand plot and the first continuum pole in the right-hand one. The jump in the trajectory of the confinement pole is due to a change of Riemann sheet at the $\phi f_0(980)$ threshold. The trajectory of the second continuum pole is depicted in Fig. 2, left-hand plot, which shows its highly non-linear and non-perturbative behaviour. As for the main purpose of the present work, we find two poles in the energy region 2.0–2.4 GeV relevant for the $X(2175)$, namely at $\boldsymbol{(2.037 - i0.170)}$ GeV and $\boldsymbol{(2.382 - i0.020)}$ GeV, being both continuum poles. The $4\,^3S_1$ ($n=3$) confinement pole can be easily followed from $E = 2.441$ GeV, up to a value of $\lambda \approx 3.1\ \text{GeV}^{-3/2}$, but one loses its track when switching Riemann sheet at the opening of the $\phi f_1(1420)$ channel. In any case, all these precise pole positions are not so important for this first study. Suffice it to say that dynamical poles can be generated in the energy region pertinent to the $X(2175)$, and possibly with quite small imaginary parts. For a very recent and more complete calculation, including the $^3D_1$ states, see Ref. [12].

[1] These results are slightly different from the preliminary ones presented at the workshop, due to a, now corrected, minor error in the computer code.

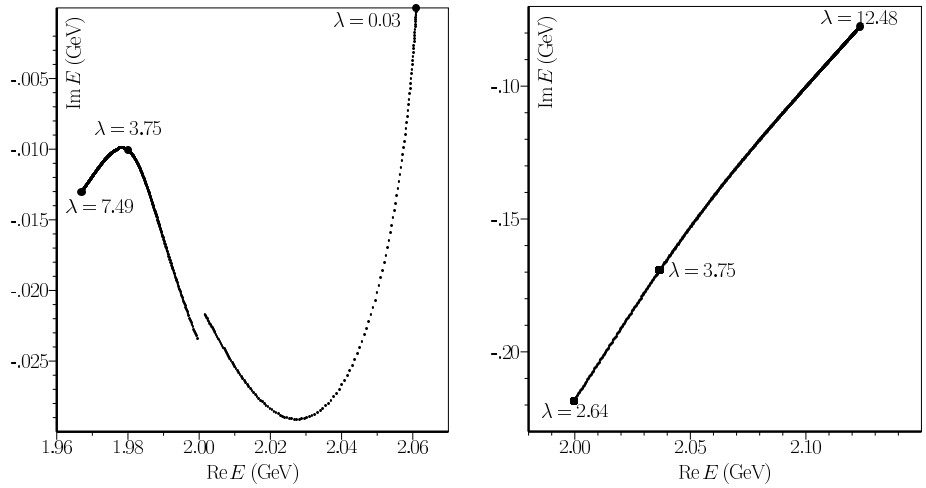

Fig. 1. Confinement pole for $3\,^3S_1$ state (left); first continuum pole (right).

Having the exact T-matrix at our disposal, we can easily compute observables, too, like cross-sections and phase shifts. Although this is not of great importance here, in view of the rather tentative pole positions above 2 GeV, we show in Fig. 2, right-hand plot, the S-wave $K^*K_1(1270)$ cross-section, just as an illustration. The pole at $(2.382 - i0.020)$ GeV is clearly visible here, in contrast with the $\phi f_0(980)$ channel. Inclusion of the $^3D_1$ states turns out to significantly improve the description, both for the pole positions and for the $\phi f_0(980)$ cross-section [12], in line with experiment.

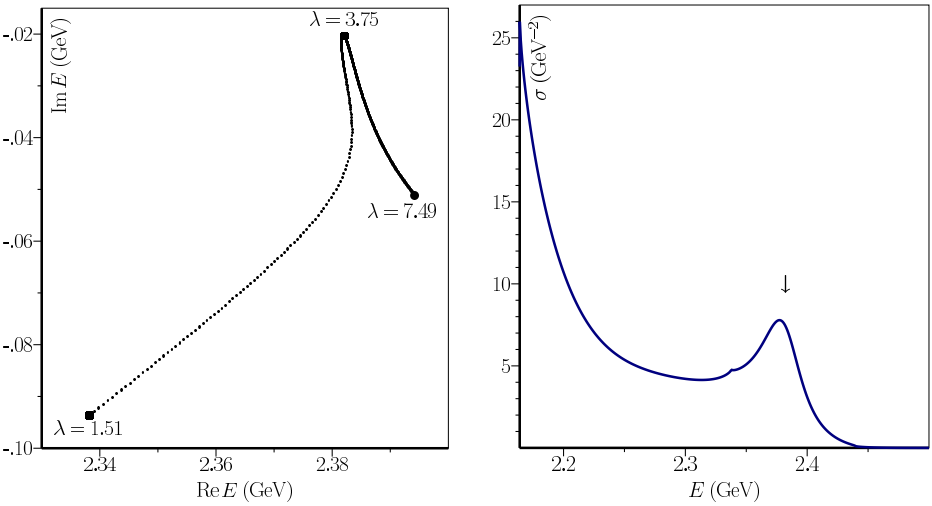

Fig. 2. Second continuum pole (left); elastic $K^*K_1(1270)$ cross-section (right).

4. Conclusions and outlook

We have shown that coupling a spectrum of confined $s\bar{s}$ states to all S-wave and P-wave two-meson channels composed of light mesons allows to generate dynamical resonances above 2 GeV, besides roughly reproducing the mass and the width of the $\phi(1020)$. This may provide a framework to understand the puzzling $X(2175)$ meson, owing to the large and non-linear coupled-channel effects, especially from the S-wave channels. Inclusion of the $^3D_1$ $s\bar{s}$ states will then account for a more realistic modelling, as confirmed by very recent results [12]. Further improvements may be considered as well, such as deviations from ideal mixing, smearing out resonances in the final state, and more general transition potentials.

We thank the organisers for an inspiring and pleasant workshop. We are also indebted to K. Khemchandani for very useful discussions. This work was supported in part by the Fundação para a Ciência e a Tecnologia of the *Ministério da Ciência, Tecnologia e Ensino Superior* of Portugal, under the contract CERN-FP-83502-2008.

Note added in proofs:
Very recent work of ours [12] revealed that the dependence of the coupling constants in Eq. (1) on the radial quantum number n was not properly normalised, resulting in too large coupled-channel effects for some higher excited states, including the $X(2175)$.

REFERENCES

[1] [BABAR Collaboration] B. Aubert *et al.*, *Phys. Rev.* **D74**, 091103 (2006).
[2] [BES Collaboration] M. Ablikim *et al.*, *Phys. Rev. Lett.* **100**, 102003 (2008).
[3] [Particle Data Group] C. Amsler *et al.*, *Phys. Lett.* **B667**, 1 (2008).
[4] A. Martinez Torres, K.P. Khemchandani, L.S. Geng, M. Napsuciale, E. Oset, *Phys. Rev.* **D78**, 074031 (2008).
[5] M. Napsuciale, E. Oset, K. Sasaki, C.A. Vaquera-Araujo, *Phys. Rev.* **D76**, 074012 (2007).
[6] Z.G. Wang, *Nucl. Phys.* **A791**, 106 (2007); H.X. Chen, X. Liu, A. Hosaka, S.L. Zhu, *Phys. Rev.* **D78**, 034012 (2008).
[7] G.J. Ding, M.L. Yan, *Phys. Lett.* **B657**, 49 (2007).
[8] E. van Beveren, G. Rupp, *Int. J. Theor. Phys. Group Theor. Nonlin. Opt.* **11**, 179 (2006).
[9] E. van Beveren, G. Rupp, *Ann. Phys.* **324**, 1620 (2009).
[10] E. van Beveren, *Z. Phys.* **C21**, 291 (1984).
[11] E. van Beveren, G. Rupp, T.A. Rijken, C. Dullemond, *Phys. Rev.* **D27**, 1527 (1983).
[12] S. Coito, E. van Beveren, G. Rupp, `arXiv:0909.0051[hep-ph]`.